DESY 13-177 ISSN 0418-9833

Inclusive charmed-meson production from bottom hadron decays at the LHC.

Paolo Bolzoni* and Gustav Kramer†

II. Institut für Theoretische Physik, Universität Hamburg,

Luruper Chaussee 149, 22761 Hamburg, Germany

(Dated: October 8, 2013)

Abstract

We present predictions for the inclusive productions of the D meson originating from bottom hadrons at the CERN LHC in the general-mass variable-flavour-number scheme at next-to-leading order. We present results using two methods to describe the transition for $b \to D$: a two-step transition $b \to B \to D$, based on the $b \to B$ fragmentation functions and the spectra for $B \to D$ as measured by CLEO and a one-step transition based on the fragmentation functions for $b \to D$. The results of both approaches are compared.

PACS numbers: 12.38.Bx, 13.85.Ni, 13.87.Fh, 14.40.Lb

*Electronic address: paolo.bolzoni@desy.de

†Electronic address: gustav.kramer@desy.de

I. INTRODUCTION

The study of heavy flavour (charm or bottom) production in proton-proton collisions at the LHC (Large Hadron Collider) is an important testing ground for perturbative QCD calculations in a new energy domain.

Charmed hadrons may be produced in pp collisions either directly or as feed-down from the decay of excited charm resonances. They may also be produced in weak decays of b-hadrons. The first two sourses (direct production and feed-down from higher mass resonances) are usually referred to as prompt production. Charmed particles from b-hadron decays are called secondary charmed hadrons or B-feed-down charmed hadrons.

Prompt charmed hadron production cross sections were measured in the central rapidity region ($|\eta| \leq 1$) in $p\bar{p}$ collisions at the Fermilab Tevatron collider at $\sqrt{s} = 1.96\,\text{TeV}$ [1] and in the central rapidity region ($|\eta| \leq 0.5$) in pp collisions at $\sqrt{s} = 2.76\,\text{TeV}$ [2] and at $\sqrt{s} = 7\,\text{TeV}$ [3, 4] and in the forward rapidity region ($2.0 \leq y \leq 4.5$) [5] at the CERN LHC. In addition, charmed hadron production cross section measurements in which prompt production and B-feed-down production have not been separated, were reported by the ATLAS Collaboration [6, 7] at the LHC. Perturbative calculations of these charmed hadron production cross section at next-to-leading order based on the General Mass Variable Flavour Number Scheme (GM-VFNS) [8] and on the fixed order with next-to-leading-logarithmic resummation (FONLL) [9] reproduce the measured cross sections [2–6].

It is conceivable that in the near future prompt charmed hadron production and production from weak decays of B meson could be well separated and that the production cross section for B-feed-down production could be measured. Actually in the case of inclusive lepton production from heavy hadron decays such a separation has been achieved. In two experiments the inclusive leptonic production cross section is measured separately for solely b-hadron decays [10, 11]. In particular, in the ALICE measurement [11] the production cross section of electrons from semileptonic bottom hadron decays was selected by using the information on the distance of the secondary decay vertex displaced in space from the primary collision vertex. It might be possible to apply this technique also in other decays of bottom hadrons, as for example, $B \to D + X$, where D is any charmed meson, D^0, $D^{\pm}$, $D^{*\pm}$, D^{*0} or D_s. The calculation of the charm hadron production from inclusive B decay into these charm hadron can be done in two ways. Either one uses fragmentation functions (FFs) for

the fragmentation process $b \to D + X$, where D is one of the charmed mesons. Such FFs have been constructed in the past from data on $e^+e^- \to D + X$ and will be described in more details in the next section. The other way is to calculate the inclusive cross section $p+p \to B+X$, where B is anyone of the bottom mesons B^0, B^+ and B_s or its antiparticles and then convolute this cross section with the inclusive spectrum of $B \to D + X$, which is known from measurements of the CLEO collaboration at CESR, the Cornell Electron Storage Ring [12], similar as we did for the inclusive production of leptons from semileptonic B decays [13]. For this calculation one needs the FFs for $b \to B$, which are knwon from the work in [15] and which we shall use. Instead of using the experimental information on the inclusive spectrum of $B \to D+X$ one could think of calculating this spectrum and compare it with the CLEO data [12]. First attempts in this direction have been done quite some time ago by Wirbel and Wu [14] much earlier than the CLEO data had appeared. Unfortunately this comparison of models as the one proposed in [14] to the CLEO data has not been done so far. Therefore we shall rely in our calculations on the empirical D meson spectrum from B decay as measured in [12]. After convolution with the $b \to B$ FFs one obtains the FFs for $b \to D$. This is an alternative method for calculationg these FFs, which is essentally based on the $b \to B$ FFs from e^+e^- annihilation data obtained at LEP and SLC. Of course it depends on the tagging of charmed mesons by CLEO at the $\Upsilon(4S)$ resonance as opposed to the direct measurements of these mesons performed by the LEP experiments at the Z resonance to be described in the next section.. The main difference of the two approaches is the tagging of the D mesons at the two energies, the CLEO energy at $\sqrt{s} = 10.58$ GeV versus the LEP energy $\sqrt{s} = m_Z$.

The content of this paper is as follows. In Section II we describe the input choices of parton distribution functions (PDFs) and B- and D-meson FFs. In this section we also explain how the fragmentation of B into D mesons has been obtained from the CLEO data. In Section III we present our predictions of the GM-VFN scheme for the cross sections $p + p \to B + X \to D + X^{'}$ for the four cases: D^0, $D^{\pm}$, $D^{*\pm}$ and D^{*0}. In addition we give the corresponding cross sections where the fragmentation functions $b \to D^0$, $D^{\pm}$ and $D^{*\pm}$ have been used in terms of ratios to the cross sections for prompt production based on the FFs for $c \to D^0$, $D^{\pm}$ and $D^{*\pm}$ and compare the ratios for the two approaches of calculating the inclusive D meson production cross sections from bottom quarks.

II. INPUT PDFS, FFS AND SETUP

The calculations presented in this paper are performed in the theoretical framework of the GM-VFNS approach for pp collisions which has been presented in detail in Refs. [15–17]. In this Section we describe our choice of input for the calculation of inclusive production of various D meson species originating from bottom quarks. For the ingoing protons we use the PDF set CTEQ6.6 [18] as implemented in the LHAPDF library [19]. This PDF set was obtained in the general-mass scheme using the input mass values $m_c = 1.3\,\mathrm{GeV}$, $m_b = 4.5\,\mathrm{GeV}$, and for the QCD strong coupling $\alpha_s^{(5)}(m_Z) = 0.118$. The c- and the b-quark PDFs have the starting scale $\mu_0 = m_c$ and $\mu_0 = m_b$, respectively.

The nonperturbative FFs for the transition $b \to B$ needed for the approach where D production is calculated from B decay to D mesons, were obtained by a fit to e^+e^- annihilation data from the ALEPH [20], OPAL [21] and SLD [22, 23] collaborations and have been published in [15]. The combined fit to the three data sets was done using the NLO sclae parameter $\Lambda^{(5)}_{\overline{MS}} = 227\,\mathrm{MeV}$ which corresponds to $\alpha_s^{(5)}(m_Z) = 0.1181$ adopted from [18]. Consistent with the chosen PDF, the starting scale of the $b \to B$ FF was assumed to be $\mu_0 = m_b$, while the $q, g \to B$ FFs, where q denotes the light quarks including the charm quark, are assumed to vanish at μ_0. Indeed their contribution is very small since they appear only via the evolution of the FFs to larger scales. As input we used the FFs with a simple power Ansatz which gave the best fit to the experimental data. The bottom mass in the hard scattering cross sections is $m_b = 4.5\,\mathrm{GeV}$ as it is used in the PDF CTEQ6.6 and in the FFs for $b \to B$.

For comparison with the results for the prompt production and for calculating the ratios of the various contributions, we also need the FFs for the transitions $c \to D^0$, D^+ and D^{*+} which we take from [24]. There we used the so-called Global-GM fit which includes fitting in addition to the OPAL data [25] together with the most precise data on D meson production from the CLEO Collaboration at CESR [26] and from the Belle Collaboration at KEKB [27]. The fits in [24], which by including the OPAL data from LEP1, yield also the FFs for $b \to D$.They are based on the charm mass $m_c = 1.5\,\mathrm{GeV}$, which is slightly larger than the one used in the CTEQ6.6 PDFs. The starting scale for $c \to D$ is $\mu_0 = m_c$, as it is for the $g, q \to D$ FFs, whereas for the $b \to D$ FF it is $\mu_0 = m_b$. The FFs for $b \to D$ as given in [24] are used for the second approach for the B feed-down production in pp collisions at the

LHC.

The theoretical accuracy of the theoretical prediction is estimated by calculating the cross sections with varying renormalization and factorization scales $\mu_{\rm R}$, $\mu_{\rm I}$ and $\mu_{\rm F}$, denoting the renormalization and the factorization scales of initial and final state singularities respectively. We choose the scales to be of order m_T, where m_T is the transverse mass $m_T = \sqrt{p_T^2 + m^2}$ with $m = m_b$ for the case of the bottom quark and $m = m_c$ for charm quark production. For exploiting the freedom in the choice of scales we have introduced the scale parameters ξ_i $(i = {\rm R}, {\rm I}, {\rm F})$ by $\mu_i = \xi_i m_T$. We vary as usual the values of the ξ_i's independently by a factor of two up and down while keeping any ratio of the ξ_i parameters smaller than or equal to two. The uncertainties due to the scale variation are dominant. Therefore PDF related uncertainties and variations of the bottom and charm mass are not considered.

The fragmentation of the final state partons i into D mesons ($D = D^0$,D^+,D^{*+} and D^{*0}) is calculated from the convolution

$$D_{i\to D}(x,\mu_F) = \int_x^1 \frac{dz}{z}\, D_{i\to B}\left(\frac{x}{z},\mu_F\right) \frac{1}{\Gamma_B}\frac{d\Gamma}{dz}(z,P_B). \tag{1}$$

In this formula, which is quite analogous to the formula we used for the fragmentation of partons i into leptons [13], $D_{i\to B}(x,\mu_F)$ is the nonperturbative FF determined in [15] for the transition $i \to B$, Γ_B is the total B decay width and finally $d\Gamma(z,P_B)/dz$ is the decay spectrum of $B \to D$. For a given D meson transverse momentum p_T and rapidity y, P_B is given by $P_B = |\vec{P_B}| = \sqrt{p_T^2 + m_T^2 \sinh^2 y}/z$. The decay distribution $d\Gamma/dk'_L$, where the momentum k'_L is parallel to $\vec{P_B}$ is obtained from the decay distribution in the rest system of the B meson using the formula in Eq.(3.16) in Ref.[28], where the formula was derived for the decay $B \to J/\Psi + X$ instead of $B \to D + X$. From this one obtaines $d\Gamma(z,P_B)/dz$ used in Eq.(1) with $z = k'_L/P_B$.

The momentum (p) spectra in inclusive decays $B \to D + X$ $(D = D^0, D^+, D^{*0}, D^{*+})$ have been measured as a function of $x = p/p_{\rm max}$ in [12] and they are given in graphical form in Figs. 16, 21, 25 and 33 of this reference. The data points have been read off from these figures and fitted by a simple power law in p of the form

$$f(p) = N\, p^\alpha\, (a-p)^\beta. \tag{2}$$

The function $f(p)$ is related to the partial D decay spectrum according to $d\Gamma/dp = c f(p)$. The obtained parameters c, N, α, β and $p_{\rm max}$ are collected in Table I for the four cases

Channel	$p_{\max}$[GeV]	N	α	β	a	c	$\chi^2_{\rm dof}$
$B \to D^0 X$	2.5070	4.5603	1.4502	1.5560	2.5070	0.047139	1.15
$B \to D^+ X$	2.5050	8.3427	1.5727	1.2013	2.5050	0.00098725	0.66
$B \to D^{*0} X$	2.4578	3081.4	1.2084	0.9538	2.4578	$3.3384 \cdot 10^{-5}$	0.58
$B \to D^{*+} X$	2.4568	976.3	1.7290	1.4648	2.4568	$8.3617 \cdot 10^{-5}$	0.34

TABLE I: The fitted parameters c, N, α, β and $p_{\max}$ for the various channels together with the corresponding χ^2 per degree of freedom.

$D = D^0$, D^+, D^{*0} and D^{*+}. In the last column we report also the corresponding χ^2 per degree of freedom. Integrating the fits $d\Gamma/dp$ over p in the kinematic range $0 \leq p \leq p_{\max}$ yields the branching ratios for $B \to DX$. The result for $D = D^0$, D^+, D^{*0} and D^{*+} is 0.627, 0.237, 0.260 and 0.225, respectively[1]. The corresponding numbers reported by the CLEO collaboration are 0.636 ± 0.030, 0.235 ± 0.027, 0.247 ± 0.028 and 0.239 ± 0.020, where the statistical and sytematic errors have been combined in quadrature, are in satisfactory agreement with the values obtained in our fits. In the CLEO experiment the inclusive D decays arise from a mixture of B^0 and B^+. The quality of our fits can be seen from Fig. 1 where the CLEO data together with our fits are shown for $B \to D^0$, D^+, D^{*0} and D^{*+} as a function of p. Actually, the inclusive D meson spectra as measured by CLEO are not measured in the B rest system, but produced at the $\Upsilon(4S)$ resonance mass. Since this mass (10.58 GeV) is slightly above the threshold for B meson pair production (10.56 GeV) the B mesons are not at rest and have a momentum ranging from 265 MeV up to 355 MeV. This motion smears the value of p or x relative to what it would be if the B were at rest. We studied this effect in our earlier work on the inclusive lepton spectra in B decays [13] and we found a very negligible effect on the spectra. Therefore we did not consider this effect for the inclusive D meson spectra, *i.e.* we consider our fits in Eq.(2) of the CLEO data as the spectra produced for B mesons at rest. With the parametrization of the D meson spectra known in the B rest system we calculated the D meson spectra in the moving system as a function of $k'_L = xP_B$ where k'_L is the D meson momentum that is parallel to $\vec{P_B}$ using Eq.(3.16) in [28] with M_ψ replaced by the rest mass of the respective D meson.

[1] These branching ratios are taken from the recent PDG [29] values. They are given for the decay of a mixture of B^+ and B^0 mesons.

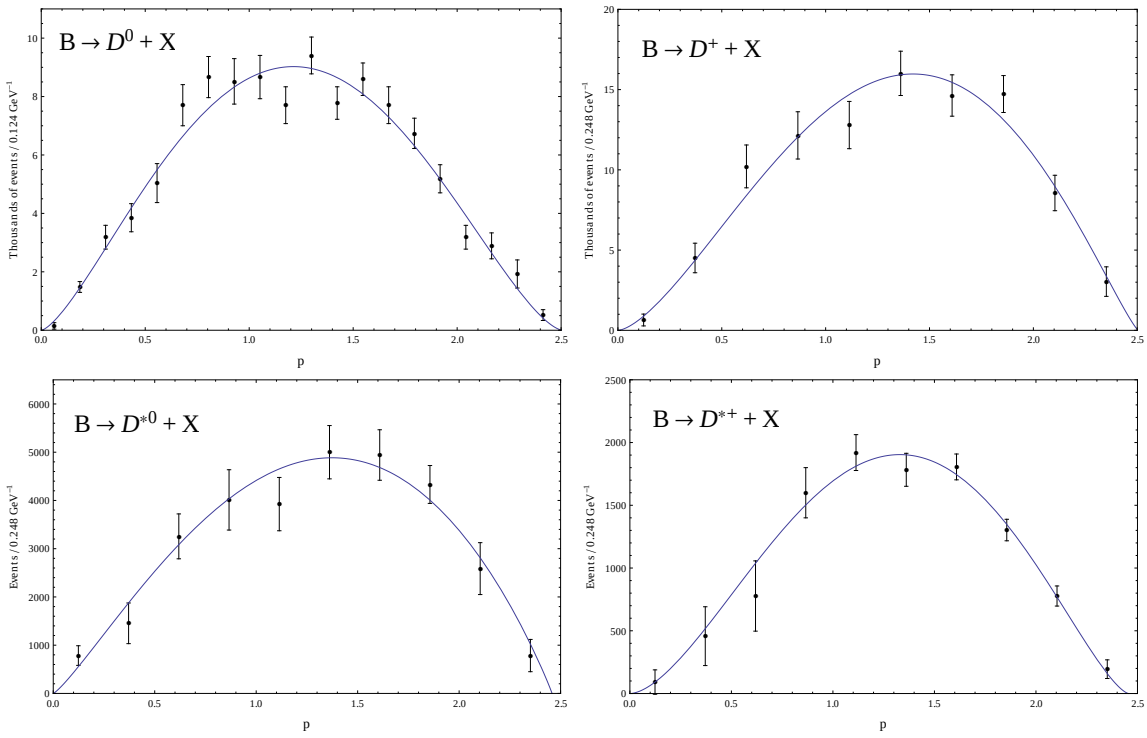

FIG. 1: Fits of data for the spectrum of the B meson decays into $D = D^0$, D^+, D^{*0} and D^{*+}.

The exact formula for $d\Gamma/dx$ as given in [28] is rather difficult to evaluate since P_B depends on p_T and the rapidity y of the produced D meson. Therefore, as in our previous work [13] we applied for $d\Gamma/dx$ the asymptotic formula, also given in [28]. This is valid for $P_B \gg M_B$, where M_B is the mass of the B meson. We calculated $d\Gamma/dx$ for various P_B and found that the exact formula differs from the asymptotic formula by less than 5% for $P_B = 15\,\mathrm{GeV}$. This is approximately achieved for $p_T = 5\,\mathrm{GeV}$ and $y = 0$ since $d\Gamma/dx$ is peaked at small $x \simeq 0.3$.

The alternative approach, which we used to calculate $d\sigma/dp_T$ for the production of D mesons originating from feed-down B meson production is the calculation with FFs for $b \to D$. Such FFs for D^0, D^+ and D^{*+} are available in [24] from fits to CLEO, Belle, OPAL and ALEPH e^+e^- annihilation data. In order to distinguish contributions originating from $c \to D$ and $b \to D$ one needs data, where the $b \to D$ contributions are separated from the total e^+e^- annihilation cross sections into charmed hadrons. This has been achieved at LEP1 at the Z resonance by the OPAL [25, 30] and the ALEPH [31] collaborations. Apart from the full cross sections, they also determined the contribution from $Z \to b\bar{b}$ decays. Using these data we have determined the FFs for $c \to X_c$ and $b \to X_c$ for charmed hadrons

$X_c = D^0$, D^+, D_s^+ and Λ_c^+ already in [32, 33] and earlier references therein. The FFs constructed in [24] have the advantage that they include the data from CLEO [26] and Belle [27] and in this way the FFs for $c \to X_c$ are much better constrained than in the earlier works [32, 33].

III. RESULTS AND COMPARISON OF THE TWO APPROACHES

In this Section we collect our results for the cross sections $d\sigma/dp_T$ as a function of p_T for the two approaches described in the previous Section. For the rapidity range we choose $-0.5 \le y \le 0.5$ as used in the ALICE experiment [2], over which the cross section $d^2\sigma/(dp_T dy)$ is integrated over. The basic formalism needed in the first approach is based on the cross section $d\sigma/dp_T$ for the inclusive production $pp \to BX$ and is described in detail in the work [34] and the references given there. In this work the inclusive B meson production cross section in $p\bar{p}$ collisions at $\sqrt{s} = 1.96$ TeV and in pp collisions was calculated and good agreement with the respective data from the CDF run II [35–37] and also with the data from the CMS Collaboration [38–40] at the LHC at $\sqrt{s} = 7$ TeV was found.

Our main results are shown in Fig. 2 (lower curves) where we present $d\sigma/dp_T$ integrated over $-0.5 \le y \le 0.5$ as a function of p_T for $3 \le p_T \le 30\,\mathrm{GeV}$ for $p + p \to D^0 X$, $(D^+ + D^-)/2\,X$, $(D^{*+} + D^{*-})/2\,X$ and $D^{*0}\,X$ for the default scale $\xi_R = \xi_I = \xi_F = 1$ (solid line) and for scales which lead to maximal and minimal cross sections (dashed lines) inside the constraints for ξ_R, ξ_I and ξ_F defined in the previous Section. The cross section for the $D^0 + X$ final state is larger than the other three due to the larger branching fractions for $B^+/B^0 \to D^0/\bar{D^0}\,X$ than, for example, for $B^+/B^0 \to D^\pm\,X$. The cross sections $d\sigma/dp_T$ for the final states $D^{*+}X$ and $D^{*0}X$ are also slightly different due to the different branching fractions for $B \to D^{*+}\,X$ and $B \to D^{*0}\,X$ and differences in the spectral shapes as can be seen in Fig. 1. Actually the results for D^0 and D^{*0} are alo for the averages of D^0 and $\overline{D^0}$ and D^{*0} and $\overline{D^{*0}}$, respectively.

In Fig. 2 we have plotted also the cross sections for $d\sigma/dp_T$ based on $c \to D^0\,X$, $D^\pm\,X$, $D^{*\pm}\,X$ and $D^{*0}\,X$, just for comparison with the corresponding feed-down B cross sections. These cross sections are the same as those presented in [8], which have been compared there to the ALICE experimental data [4]. The shapes of the two cross sections for $c \to D$ and $b \to B \to D$ are very similar, at least for the larger $p \ge 10\,\mathrm{GeV}$. This is seen more clearly in

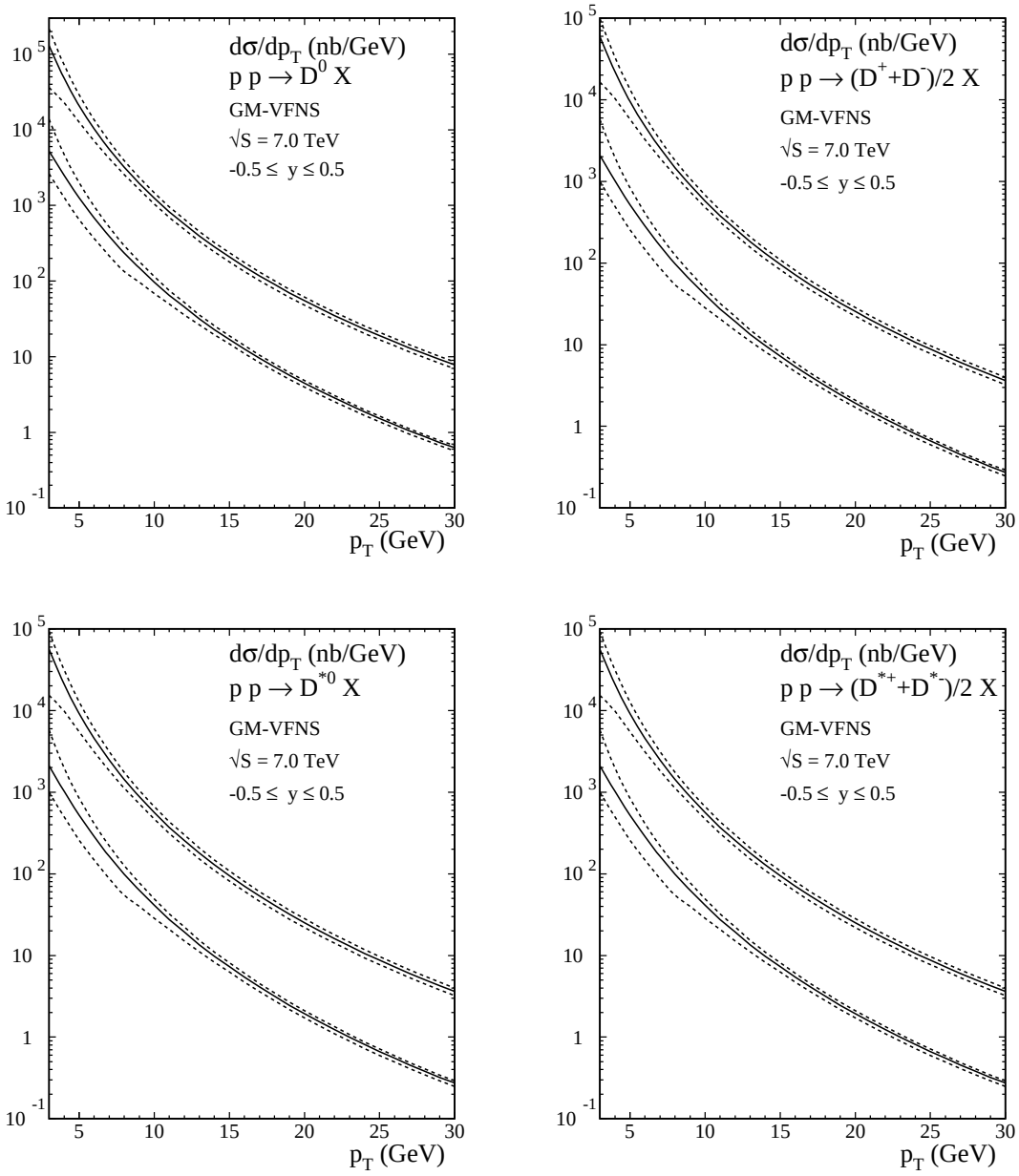

FIG. 2: The lower curves, together with the corresponding scale uncertainties (dashed lines), are our predictions for the B-feed-down hadrons ($b \to B \to D$). For comparison we also show (upper curves) the cross sections corresponding to $c \to D$.

Fig. 3 where we have plotted the ratio of $d\sigma/dp_T$ for the two cross sections (lower curves), for the default scale choice (full curve) and the maximal and minimal scale choice (dashed curves). For the latter two curves the scale variation is included only for the numerator, *i.e.* for $d\sigma/dp_T$ for $b \to B \to D$. As it can be seen, this ratio is nearly independent of p_T for

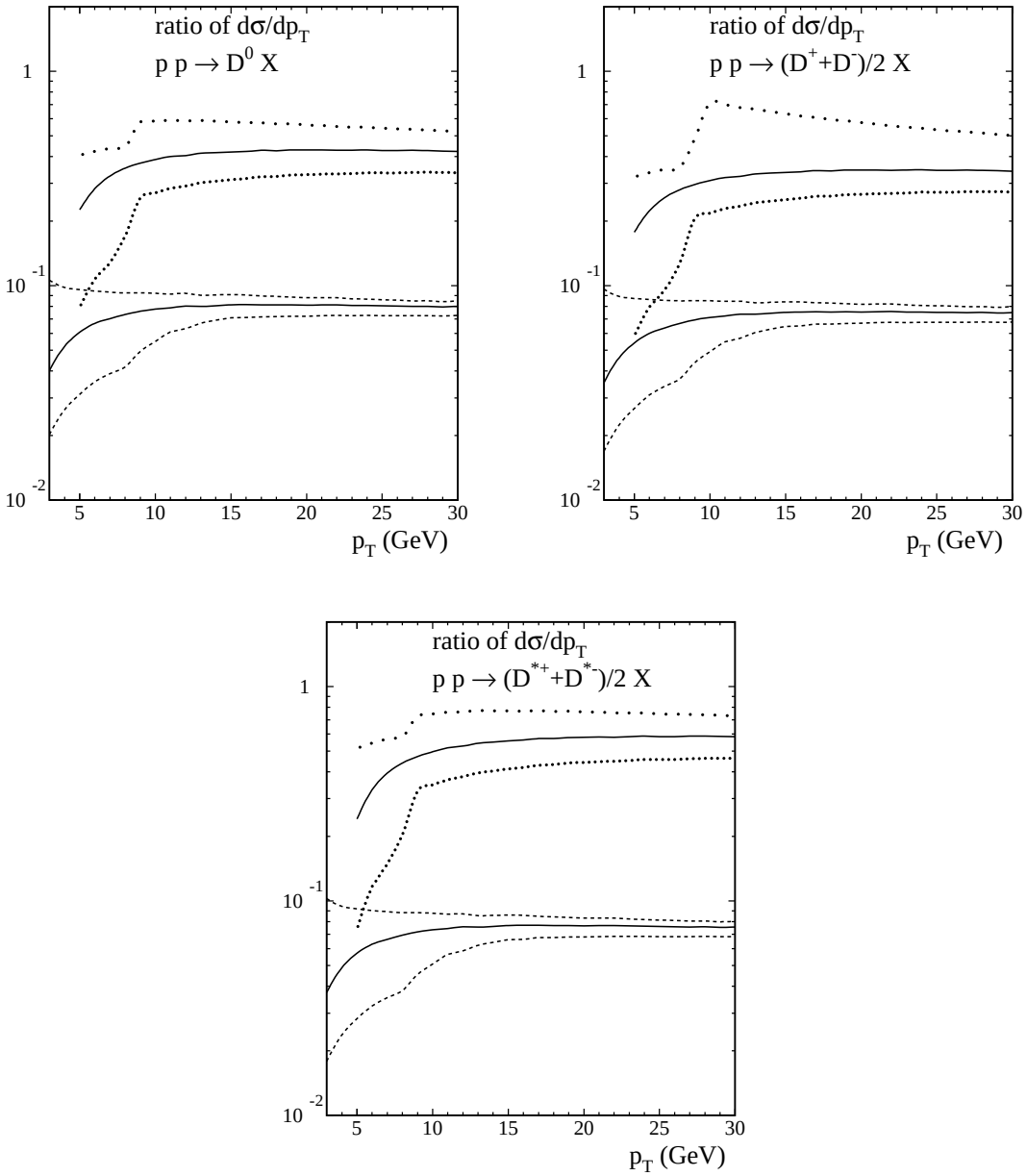

FIG. 3: Ratio of the cross section for $b \to B \to D$ (lower curves) and for $b \to D$ (upper curves) to the cross section for $c \to D$. The last ratios are multiplied by a factor of 10 for better visibility.

approximately $p_T > 10\,\mathrm{GeV}$ and is around 8.0%, 7.5% and 7.5% for the largest p_T and for the three cases D^0 ,$D^{\pm}$ and $D^{*\pm}$, respectively. For $p_T < 10\,\mathrm{GeV}$ this ratio decreases and apporaches 4% at $p_T = 3\,\mathrm{GeV}$.

The predictions for $d\sigma/dp_T$ using the one-step approach based on the fragmentation functions for $b \to D$ from [24] are given only in the form of ratios to $d\sigma/dp_T$ for $c \to D$.

These results are also shown in Fig. 3 as the upper curves: full for the default and dotted curves for the maximal and minimal result. For better visibility these ratios are multiplied by a factor 10. The shape of this ratio as a function of p_T for $5.0 < p_T < 30\,\text{GeV}$ is similar as for the case of the two-step FFs: $b \to B \to D$. The only significant differences are the absolute values of the ratios. At the largest p_T the ratios for $b \to D$ are approximately between 50% and 20% smaller than the ratios for $b \to B \to D$ shown as the lower curves in Fig. 3. The reason for this decrease is not caused by a mismatch of the branching ratios. Indeed, for example, in the case $b \to B \to D^0$ the total branching ratio is approximatel $0.8 \times 0.627 = 0.502$ in good agreement with the branching ratio for $b \to D^0$ equal to 0.515 as given in Table 11 of [24] and similarly for the other channels. Therfore the reason for the differeent ratio in the upper and lower part of Fig. 3 must lie in the shape of the FFs. The FFs in the two approaches have a similar shape of approximately gaussian form with a maximum near $z = 0.25$.

First we should ask, however, why the cross section $d\sigma/dp_T$ is so much smaller for $b \to B \to D$ than the one for $c \to D$ as already clearly seen in Fig. 2. To answer this question we calculated the average z as a function of p_T in the relevant region of p_T. This $< z > (p_T)$ is the quantity

$$< z > (p_T) = \frac{\int dz z d\sigma/dp_T}{\int dz d\sigma/dp_T} \tag{3}$$

where z is the scaling variable of the respective FFs. It is understood that the integration of the quantities of the numerator and of the denominator is done over the the rapidity interval $|y| \leq 0.5$. The range of $< z >$'s for the four cases $D^0, D^{\pm}, D^{*\pm}$ and D^{*0} is in the p_T range $3.0 \leq p_T \leq 30$ GeV equal to $< z >= [0.43, 0.48], [0.45, 0.50], [0.35, 0.45]$ and $[0.45, 0.50]$. This means that the relevant z range, where the FFs contribute to $d\sigma/dp_T$, lie outside the maximum of the FFs on the right side, where the FFs decreased already by an aprecciable factor. The FFs for $c \to D$, on the other hand, have a similar shape with a maximum at $< z > \cong 0.65$ [24], which is approximately the relevant range for $d\sigma/dp_T$. For example, for $c \to D^0$ we obtain $< z >= [0.67, 0.64]$ in the range $3 < p_T < 30$ GeV, which is just in the vicinity of the z, where the corresponding FF is maximal. From this we conclude that the smallness of the cross section $d\sigma/dp_T$ for $b \to D$'s in the considered p_T range is due to the fact that the corresponding FFs contribute only outside the range where the FF is maximal and has decreased already appreciably.

For the one-step FFs $b \to D$'s the average z ranges in the cross section $d\sigma/dp_T$ are similar

as in the two-step process. The only exception is $b \to D^{*\pm}$ where $< z >$ ranges in the interval $[0.44, 0.53]$, which is 0.1 larger than for the case $b \to B \to D^{*\pm}$., where the corresponding FF is smaller, which has the effect that the cross section $d\sigma/dp_T$ is snaller by 20% than for the two- step process as can be seen in Fig. 3. In the other two cases D^0 and $D^{\pm}$ it turns out that in the relevant region the one-step FF is smaller than the two-step FF.

IV. SUMMARY

In this paper we have calculated the cross sections $d\sigma/dp_T$ for inclusive D meson production for several D meson charge states originating from weak bottom quark decays at the LHC c.m. energy of 7 TeV in the framework of the GM-VFN scheme. We used two approches for calculating the FFs for $b \to D$. In the two-step approach: $b \to B \to D$'s we constructed the FFs based on the $b \to B$ FF fitted to B production data from LEP and SLC convoluted with FFs for $B \to D$'s obtained from measuerements of the CLEO collaboration. In the one-step approach we used FFs for $b \to D$, constructed from e^+e^- annihilation cross section for the production of D mesons from b quarks.

In both approaches the cross section for $pp \to DX$ with D's originating from b quarks decays is only a small fraction of the dominant contribution where the D mesons come from the fragmentation of charm quarks. The reason for the reduction of the $pp \to bX' \to DX$ cross sections as compared to the $pp \to cX' \to DX$ originates from the fact that in the second case the FF for $c \to D$'s contributes in the region of fractional momenta, where the FF is maximal, whereas in the first case the contributing region of the FF is above the maximal region where the FF has decreased aprecciably. The difference in the cross sections for the one-step and two-step approaches can be explained by the stronger fall-off of the FFs from the one-step approach above the z's where the maximum occurs. Therfore the measurement of the cross section for D meson production from b decays at the LHC is an ideal place to get information on the behaviour of the FFs for $b \to D$'s beyond where the maximun occurs.

Acknowledgments

We thank H. Spiesberger for help with the modification of the GM-VFNS cross section routine. This work was supported in part by the German Federal Ministry for Education and Research BMBF through Grant No. 05 H12GUE, by the German Research Foundation DFG through Grant No. KN 365/7–1, and by the Helmholtz Association HGF through Grant No. Ha 101.

---

[1] D. Acosta et al. (CDF Collaboration), Phys.Rev.Lett. **91**, 241804 (2003), hep-ex/0307080.

[2] B. Abelev et al. (ALICE Collaboration), JHEP **1207**, 191 (2012), 1205.4007.

[3] B. Abelev et al. (ALICE Collaboration), Phys.Lett. **B718**, 279 (2012), 1208.1948.

[4] B. Abelev et al. (ALICE Collaboration), JHEP **1201**, 128 (2012), 1111.1553.

[5] R. Aaij et al. (LHCb collaboration), Nucl.Phys. **B871**, 1 (2013), 1302.2864.

[6] ATLAS Collaboration, ATL-PHYS-PUB-2011-012, ATL-COM-PHYS-2011-912 (2011).

[7] ATLAS Collaboration, ATLAS-CONF-2011-017, ATLAS-COM-CONF-2011-030 (2011).

[8] B. Kniehl, G. Kramer, I. Schienbein, and H. Spiesberger, Eur.Phys.J. **C72**, 2082 (2012), 1202.0439.

[9] M. Cacciari, S. Frixione, N. Houdeau, M. L. Mangano, P. Nason, et al., JHEP **1210**, 137 (2012), 1205.6344.

[10] V. Khachatryan et al. (CMS Collaboration), JHEP **1103**, 090 (2011), 1101.3512.

[11] B. Abelev et al. (ALICE Collaboration), Phys.Lett. **B721**, 13 (2013), 1208.1902.

[12] L. Gibbons et al. (CLEO Collaboration), Phys.Rev. **D56**, 3783 (1997), hep-ex/9703006.

[13] P. Bolzoni and G. Kramer, Nucl.Phys. **B872**, 253 (2013), 1212.4356.

[14] M. Wirbel and Y. L. Wu, Phys.Lett. **B228**, 430 (1989).

[15] B. A. Kniehl, G. Kramer, I. Schienbein, and H. Spiesberger, Phys.Rev. **D77**, 014011 (2008), 0705.4392.

[16] B. Kniehl, G. Kramer, I. Schienbein, and H. Spiesberger, Phys.Rev. **D71**, 014018 (2005), hep-ph/0410289.

[17] B. Kniehl, G. Kramer, I. Schienbein, and H. Spiesberger, Eur.Phys.J. **C41**, 199 (2005), hep-ph/0502194.

[18] P. M. Nadolsky, H.-L. Lai, Q.-H. Cao, J. Huston, J. Pumplin, et al., Phys.Rev. **D78**, 013004 (2008), 0802.0007.

[19] M. Whalley, and D. Bourilkov, (2005), hep-ph/0508110.

[20] A. Heister et al. (ALEPH Collaboration), Phys.Lett. **B512**, 30 (2001), hep-ex/0106051.

[21] G. Abbiendi et al. (OPAL Collaboration), Eur.Phys.J. **C29**, 463 (2003), hep-ex/0210031.

[22] K. Abe et al. (SLD Collaboration), Phys.Rev.Lett. **84**, 4300 (2000), hep-ex/9912058.

[23] K. Abe et al. (SLD Collaboration), Phys.Rev. **D65**, 092006 (2002); **D66**, 079905(E) (2002), hep-ex/0202031.

[24] T. Kneesch, B. Kniehl, G. Kramer, and I. Schienbein, Nucl.Phys. **B799**, 34 (2008), 0712.0481.

[25] G. Alexander et al. (OPAL Collaboration), Z.Phys. **C72**, 1 (1996).

[26] M. Artuso et al. (CLEO Collaboration), Phys.Rev. **D70**, 112001 (2004), hep-ex/0402040.

[27] R. Seuster et al. (Belle Collaboration), Phys.Rev. **D73**, 032002 (2006), hep-ex/0506068.

[28] B. A. Kniehl and G. Kramer, Phys.Rev. **D60**, 014006 (1999), hep-ph/9901348.

[29] J. Beringer et al. (Particle Data Group), Phys.Rev. **D86**, 010001 (2012).

[30] K. Ackerstaff et al. (OPAL Collaboration), Eur.Phys.J. **C1**, 439 (1998), hep-ex/9708021.

[31] R. Barate et al. (ALEPH Collaboration), Eur.Phys.J. **C16**, 597 (2000), hep-ex/9909032.

[32] B. A. Kniehl and G. Kramer, Phys.Rev. **D71**, 094013 (2005), hep-ph/0504058.

[33] B. A. Kniehl and G. Kramer, Phys.Rev. **D74**, 037502 (2006), hep-ph/0607306.

[34] B. Kniehl, G. Kramer, I. Schienbein, and H. Spiesberger, Phys.Rev. **D84**, 094026 (2011), 1109.2472.

[35] D. Acosta et al. (CDF Collaboration), Phys.Rev. **D71**, 032001 (2005), hep-ex/0412071.

[36] T. Aaltonen et al. (CDF Collaboration), Phys.Rev. **D79**, 092003 (2009), 0903.2403.

[37] A. Abulencia et al. (CDF Collaboration), Phys.Rev. **D75**, 012010 (2007), hep-ex/0612015.

[38] V. Khachatryan et al. (CMS Collaboration), Phys.Rev.Lett. **106**, 112001 (2011), 1101.0131.

[39] S. Chatrchyan et al. (CMS Collaboration), Phys.Rev.Lett. **106**, 252001 (2011), 1104.2892.

[40] S. Chatrchyan et al. (CMS Collaboration), Phys.Lett. **B714**, 136 (2012), 1205.0594.